On computing stress in polymer systems involving multi-body potentials from molecular dynamics simulation

Yao Fu[a),b)] and Jeong-Hoon Song[a)]
Department of Civil, Environmental, and Architectural Engineering, University of Colorado, Boulder, Colorado 80309, USA

(Received 23 April 2014; accepted 18 July 2014; published online 5 August 2014)

Hardy stress definition has been restricted to pair potentials and embedded-atom method potentials due to the basic assumptions in the derivation of a symmetric microscopic stress tensor. Force decomposition required in the Hardy stress expression becomes obscure for multi-body potentials. In this work, we demonstrate the invariance of the Hardy stress expression for a polymer system modeled with multi-body interatomic potentials including up to four atoms interaction, by applying central force decomposition of the atomic force. The balance of momentum has been demonstrated to be valid theoretically and tested under various numerical simulation conditions. The validity of momentum conservation justifies the extension of Hardy stress expression to multi-body potential systems. Computed Hardy stress has been observed to converge to the virial stress of the system with increasing spatial averaging volume. This work provides a feasible and reliable linkage between the atomistic and continuum scales for multi-body potential systems. © *2014 AIP Publishing LLC*. [http://dx.doi.org/10.1063/1.4891606]

I. INTRODUCTION

For decades, continuum mechanics has been widely used to predict averaged materials response and failure in the macroscopic length scale. As the origins of macroscopic behaviors reside in the material behaviors at the finer scale, there is a growing need to obtain a more fundamental understanding of the material deformation mechanism. On the other hand, atomistic simulations allows for studying material behaviors at the atomistic scale by using interatomic potentials fitted from *ab initio* calculations and/or physical measurements of materials properties. Atomistic simulation can display the microscopic deformation mechanism such as dislocation nucleation and propagation, shear bands formation, and micro-voids nucleation and growth. However, the high computational expense prohibits the analysis of micro-scale systems using fully atomistic modeling even with the rapid development of large-scale parallel computing techniques. Therefore, it is natural to develop coupled atomistic-continuum methods to combine the strength of atomistic and continuum modeling.[1–9] In the hierarchical atomistic-continuum modeling, results from atomistic simulations can be employed to build constitutive laws, which serve as an input to the continuum mechanics modeling. Concurrent multi-scale modeling involves problems where two or more length and/or time scale play roles in the overall mechanical behaviors. Information transfer between the atomistic and continuum scales is vital in the process of multi-scale modeling. Therefore, defining continuum quantities in terms of atomistic quantities is of both theoretical and practical significance.

Interests in the microscopic definitions of stress tensor dated back to the work by Clausius[10] and Maxwell[11,12] in the form of virial theorem. The virial stress resulting from this theorem is a macroscopic average stress and has been widely used in atomistic simulations due to its simple form and ease of computation. Alternatively, Irving and Kirkwood[13] developed stress tensor in their classical paper on the equations of hydrodynamics; they proposed formulas for mass, momentum, and energy densities in terms of atomistic quantities. The pointwise definitions of stress tensor and heat flux vector are established through the principles of non-equilibrium classical statistical mechanics. However, the stress definition involves an infinite series expansion of the Dirac delta function which needs to be approximated during the computations; i.e., atomistic simulations. Moreover, Irving and Kirkwook formulas considered the stochastic nature of dynamic processes and thus needs knowledge of a probability density distribution function of the dynamic ensemble which is usually not known *a priori*. Therefore, these formulas are difficult to be implemented for atomistic simulations despite their remarkable theoretical contributions. To avoid the complexities in Irving and Kirkwood's work, Hardy and co-workers,[14,15] and Murdoch[16–20] independently developed stress definitions by direct spatial averaging of the atomistic equation of motion using a normalized weighting function. As a consequence, the so-called Hardy stress is often used in current atomistic simulations.[21–27]

However, Hardy made key assumptions on the forms of energies and forces for the atomic system to derive the expression for a symmetric stress tensor: (1) The force on atom i can be expressed as the summation $\mathbf{f}^i = \sum_{j \neq i} \mathbf{f}^{ij}$, where $\mathbf{f}^{ij}$ is the force on atom i from atom j and satisfies $\mathbf{f}^{ij} = -\mathbf{f}^{ji}$; (2) The interatomic potential energies depend only on the interatomic distance between the atom under consideration

a)Authors to whom correspondence should be addressed. Electronic addresses: fu5@mailbox.sc.edu and jhsong@cec.sc.edu
b)Post-doctoral Fellow.

and all other atoms. So far, Hardy stress has been mostly used to compute stress for atomistic systems modeled by pair and embedded-atom method (EAM) potentials[21–24] because these assumptions have not been proved to hold for general multi-body potentials. Chen[28] discussed the possibility of extending Hardy stress expression to systems involving three-body potentials such as Tersoff[29] and Stillinger-Weber potentials.[30] Chen demonstrated the invariance of Hardy stress formula for three-body systems if $\mathbf{f}^{ij}$ is defined as $\mathbf{f}^{ij} := -\partial E_V/\partial \mathbf{r}^{ij}$, where E_V is the total potential energy of the system and $\mathbf{r}^{ij} = \mathbf{r}^i - \mathbf{r}^j$, $\mathbf{r}^i$ denotes the position of atom i. Admal *et al.*[31,32] addressed the force decomposition problem for multi-body potentials, with the key result that the force on a particle can always be decomposed as a sum of central forces between particles for most practical interatomic potentials. Various forms of the force decomposition can possibly exist due to the non-uniqueness of the interatomic potential extension for an N particle system with $N \geq 5$.[31,32] With central force decomposition, the assumptions in Hardy's derivation can be satisfied for multi-body systems modeled by most practical interatomic potentials.

In this study, we aim to extend the Hardy stress expression to multi-body potential systems based on the work of Admal *et al.*[31,32] and Chen.[28] We use a typical coarse-grained (CG) model for polyethylene (PE) polymer system, which involves up to four-body potential, as an example to demonstrate the invariance of Hardy stress expression to multi-body potential system both theoretically and numerically. In Sec. II, force decomposition expression proposed by Admal *et al.*[31,32] is applied to the polymer system. In Sec. III, the invariance of Hardy stress expression is demonstrated for the system involving up to four body interatomic potentials. This is followed by computing Hardy stress from a variety of molecular dynamics conditions: unstrained and strained polymer of different chain length at glassy and melt states in Sec. IV. Hardy's density, velocity, and stress expressions for the polymer system have also been shown to obey the balance of momentum numerically.

II. FORCE DECOMPOSITION FOR MULTI-BODY POTENTIALS

The interatomic potentials used for coarse-grained (CG) polymer systems typically include bond stretching between adjacent superatoms, bending deformation in terms of a bond angle θ, torsional deformation in terms of a dihedral angle ϕ, and non-bonded interaction described by the Lennard-Jones (LJ) potential. For example, the potentials listed in Eq. (2.1) are widely applied to model CG polymer systems:[33,34]

$$V_b(r^{ij}) = k_b(r^{ij} - r_0)^2, \tag{2.1a}$$

$$V_\theta(r^{ij}, r^{ik}, r^{jk}) = k_\theta\left(\frac{\mathbf{r}^{ij}\cdot\mathbf{r}^{kj}}{r^{ij}r^{kj}} - \cos\theta_0\right)^2 = k_\theta(\cos\theta^{ijk} - \cos\theta_0)^2, \tag{2.1b}$$

$$V_\phi(r^{ij}, r^{ik}, \ldots r^{kl}) = c_0 + c_1\cos\phi^{ijkl} + c_2\cos^2\phi^{ijkl} + c_3\cos^3\phi^{ijkl} + c_4\cos^4\phi^{ijkl},$$
$$\cos\phi^{ijkl} = \frac{-\cos\theta^{kl,ij} + cos\theta^{kl,jk}cos\theta^{jk,ij}}{\sin\theta^{kl,jk}\sin\theta^{jk,ij}},$$
$$\cos\theta^{ij,kl} = \frac{\mathbf{r}^{ij}\cdot\mathbf{r}^{kl}}{r^{ij}r^{kl}}, \tag{2.1c}$$

$$V_{LJ}(r^{ij}) = 4\varepsilon\left[\left(\frac{\sigma}{r^{ij}}\right)^{12} - \left(\frac{\sigma}{r^{ij}}\right)^{6}\right], \tag{2.1d}$$

where V_b, V_θ, V_ϕ, and V_{LJ} denotes potential energy contribution from bond stretching, bending, torsional, and non-bonded interaction, respectively. $r^{ij} = \|\mathbf{r}^{ij}\|$ is the length of the vector $\mathbf{r}^{ij}$, $\mathbf{r}^{ij} = \mathbf{r}^i - \mathbf{r}^j$, $\mathbf{r}^i$ denotes the position of atom i. $\cos\theta^{ij,kl} = \frac{\mathbf{r}^{ij}\cdot\mathbf{r}^{kl}}{r^{ij}r^{kl}}$ denotes the angle formed by the two vectors $\mathbf{r}^{ij}$ and $\mathbf{r}^{kl}$. k_b is the constant for bond stretching potential and r_0 is the equilibrium bond length. k_θ is the constant of the bond bending potential and θ_0 is the equilibrium bond angle. c_n ($n = 0, 1, 2, 3, 4$) are the constants of torsional potential. ε represents the interaction strength and σ determines the minimum energy position of LJ potential.

The interatomic potential energy, E_V, is a sum of contributions from the two-body (stretching and non-bonded), three-body (bending), and four-body (torsional) interactions:

$$E_V = \frac{1}{2!}\sum_i\sum_{j\neq i}\{V_b(r^{ij}) + V_{LJ}(r^{ij})\} + \frac{1}{3!}\sum_i\sum_{j\neq i}\sum_{k\neq i,j}V_\theta(r^{ij}, r^{ik}, r^{jk})\ldots + \frac{1}{4!}\sum_i\sum_{j\neq i}\sum_{k\neq i,j}\sum_{l\neq i,j,k}V_\phi(r^{ij}, r^{ik}, r^{jk}, \ldots, r^{kl}). \tag{2.2}$$

A more general form of the total potential energy, E_V, for a multi-body potential system is[35,36]

$$E_V = \frac{1}{2!}\sum_i\sum_{j\neq i}V_2(r^{ij}) + \frac{1}{3!}\sum_i\sum_{j\neq i}\sum_{k\neq i,j}V_3(r^{ij}, r^{ik}, r^{jk})\ldots + \ldots + \frac{1}{N!}\sum_i\sum_{j\neq i}\sum_{k\neq i,j}\cdots\sum_{q\neq i,j,k,\ldots p}V_N(r^{ij}, r^{ik}, r^{jk}, \ldots, r^{pq}). \tag{2.3}$$

As mentioned by Admal *et al.*,[31,32] the force on the ith particle can always be decomposed as a sum of central forces as long as the interatomic potential energy, E_V, defined on shape space $\mathcal{S} := \{r^{12}, r^{13}, \ldots, r^{1N}, r^{23}, \ldots, r^{(N-1)N}\}$, are continuously differentiable, which is apparently applicable to the interatomic potentials used here. According to the

chain rule

$$\mathbf{f}^i = -\frac{\partial E_V}{\partial \mathbf{r}^i} = -\sum_j \frac{\partial E_V}{\partial r^{ij}} \frac{\mathbf{r}^{ij}}{r^{ij}} = \sum_j \mathbf{f}^{ij}, \tag{2.4}$$

where $\mathbf{f}^{ij}$ is defined as

$$\mathbf{f}^{ij} := -\frac{\partial E_V}{\partial r^{ij}} \frac{\mathbf{r}^{ij}}{r^{ij}} = -\frac{\partial E_V}{\partial \mathbf{r}^{ij}}. \tag{2.5}$$

It is easy to verify that $\mathbf{f}^{ij}$ defined as such naturally satisfies $\mathbf{f}^i = \sum_j \mathbf{f}^{ij}$ from Eq. (2.4) and is parallel to $\mathbf{r}^{ij}$ as required by the strong law of action and reaction, thus is called the central force. The central force decomposition has been justified to be the only physically meaningful way to decompose $\mathbf{f}^i$.[31]

From Eqs. (2.3) and (2.5), the force on the ith atom due to the presence of jth atom can be obtained as

$$\begin{aligned}
\mathbf{f}^{ij} &:= -\frac{\partial E_V}{\partial r^{ij}} \frac{\mathbf{r}^{ij}}{r^{ij}} \\
&= -\left(\begin{array}{l} \frac{1}{2!} \sum_k \sum_{l\neq k} \frac{\partial V_2(r^{kl})}{\partial r^{ij}} \cdots \\ +\frac{1}{3!} \sum_k \sum_{l\neq k} \sum_{m\neq k,l} \frac{\partial V_3(r^{kl}, r^{km}, r^{lm})}{\partial r^{ij}} \cdots \\ +\ldots+\frac{1}{N!} \sum_k \sum_{l\neq k} \sum_{m\neq k,l} \cdots \sum_{q\neq k,l,m,..p} \frac{\partial V_N(r^{kl}, r^{km}, r^{lm}, \ldots r^{pq})}{\partial r^{ij}} \end{array} \right) \frac{\mathbf{r}^{ij}}{r^{ij}} \\
&= -\left(\begin{array}{l} \frac{1}{2!} \sum_k \sum_{l\neq k} \frac{\partial V_2}{\partial r^{ij}} (\delta_{ik}\delta_{jl} + \delta_{il}\delta_{jk}) \cdots \\ +\frac{1}{3!} \sum_k \sum_{l\neq k} \sum_{m\neq k,l} \frac{\partial V_3}{\partial r^{ij}} \left(\delta_{ik}\delta_{jl} + \delta_{il}\delta_{jk} + \delta_{ik}\delta_{jm} + \delta_{im}\delta_{jk} + \delta_{il}\delta_{jm} + \delta_{im}\delta_{jl}\right) \cdots \\ +\ldots+\frac{1}{N!} \sum_k \sum_{l\neq k} \sum_{m\neq k,l} \cdots \sum_{q\neq k,l,m,..p} \frac{\partial V_N}{\partial r^{ij}} \left(\delta_{ik}\delta_{jl} + \delta_{il}\delta_{jk} + \ldots + \delta_{iq}\delta_{jp} + \delta_{ip}\delta_{jq}\right) \end{array} \right) \frac{\mathbf{r}^{ij}}{r^{ij}} \\
&= \mathbf{f}_2^{ij} + \sum_k \mathbf{f}_3^{ij} + \ldots + \frac{\mathrm{N(N-1)}}{\mathrm{N!}} \sum_k \sum_{l\neq k} \sum_{m\neq k,l} \cdots \sum_{h\neq k,l,m,\ldots g} \mathbf{f}_N^{ij},
\end{aligned} \tag{2.6a}$$

$$\mathbf{f}_N^{ij} := -\frac{\partial V_N}{\partial r^{ij}} \frac{\mathbf{r}^{ij}}{r^{ij}} = -\frac{\partial V_N}{\partial \mathbf{r}^{ij}} \tag{2.6b}$$

For the PE polymer simulated by the CG model in our study,

$$\mathbf{f}^{ij} = \mathbf{f}_{stretch}^{ij} + \mathbf{f}_{LJ}^{ij} + \sum_k \mathbf{f}_{bend}^{ij} + \ldots + \frac{1}{2} \sum_k \sum_{l\neq k} \mathbf{f}_{torsion}^{ij}, \tag{2.7}$$

where the derivation of $\mathbf{f}_{bend}^{ij}$ and $\mathbf{f}_{torsion}^{ij}$ can be found in the Appendix.

III. HARDY STRESS FOR POLYMER SYSTEMS INVOLVING MULTI-BODY POTENTIALS

Hardy's formulas define mass density, $\rho(\mathbf{x}, t)$, and momentum density, $\mathbf{p}(\mathbf{x}, t)$, fields in the continuum spatial point, $\mathbf{x}$, and time instant, t, in terms of a localization function $\psi(\mathbf{x})$,

$$\rho(\mathbf{x}, t) = \sum_i m^i \psi(\mathbf{r}^i - \mathbf{x}), \tag{3.1a}$$

$$\mathbf{p}(\mathbf{x}, t) = \sum_i m^i \mathbf{v}^i \psi(\mathbf{r}^i - \mathbf{x}), \tag{3.1b}$$

$$\mathbf{v}(\mathbf{x}, t) = \frac{\mathbf{p}(\mathbf{x}, t)}{\rho(\mathbf{x}, t)}, \tag{3.1c}$$

where m^i and $\mathbf{v}^i$ denote the mass and velocity, respectively, of atom i, and $\mathbf{v}(\mathbf{x}, t)$ is the local velocity in the continuum spatial point, $\mathbf{x}$, at a time instant t.

Taking the partial time derivative of momentum density (3.1b),

$$\begin{aligned}
\frac{\partial \mathbf{p}(\mathbf{x}, t)}{\partial t} &= \sum_i m^i \frac{\mathrm{d}\mathbf{v}^i}{\mathrm{d}t} \psi(\mathbf{r}^i - \mathbf{x}) + m^i \mathbf{v}^i \frac{\partial \psi(\mathbf{r}^i - \mathbf{x})}{\partial t} \\
&= \sum_i \mathbf{f}^i \psi(\mathbf{r}^i - \mathbf{x}) + m^i \mathbf{v}^i \frac{\partial \psi(\mathbf{r}^i - \mathbf{x})}{\partial \mathbf{r}^i} \cdot \mathbf{v}^i,
\end{aligned} \tag{3.2}$$

where $\mathbf{f}^i = -\frac{\partial E_V}{\partial \mathbf{r}^i}$ is the interatomic force on atom i, and the body force from gravity or electromagnetic fields are assumed

negligible. In the original Hardy's derivation for pair potential system, $\mathbf{f}^i$ can be easily written as $\mathbf{f}^i = \sum_{j\neq i} \mathbf{f}^{ij}$ and $\mathbf{f}^{ij} = -\mathbf{f}^{ji}$ is satisfied. The physical meaning of $\mathbf{f}^{ij}$ for the pair potential system is clearly the force on atom i from atom j. Even though it is not so straightforward to explain the meaning of $\mathbf{f}^{ij}$ for multi-body potential systems, the results from Sec. II ensures that $\mathbf{f}^i = \sum_{j\neq i} \mathbf{f}^{ij}$ and $\mathbf{f}^{ij} = -\mathbf{f}^{ji}$ are satisfied if $\mathbf{f}^{ij}$ is defined as $\mathbf{f}^{ij} := -\frac{\partial E_V}{\partial r^{ij}}\frac{\mathbf{r}^{ij}}{r^{ij}} = -\frac{\partial E_V}{\partial \mathbf{r}^{ij}}$. Using $\mathbf{f}^i = \sum_{j\neq i} \mathbf{f}^{ij}$, Eq. (3.2) becomes

$$\sum_i \mathbf{f}^i \psi(\mathbf{r}^i - \mathbf{x}) + m^i \mathbf{v}^i \frac{\partial \psi(\mathbf{r}^i - \mathbf{x})}{\partial \mathbf{r}^i} \cdot \mathbf{v}^i = \sum_i \sum_{j\neq i} \mathbf{f}^{ij} \psi(\mathbf{r}^i - \mathbf{x}) + m^i \mathbf{v}^i \frac{\partial \psi(\mathbf{r}^i - \mathbf{x})}{\partial \mathbf{r}^i} \cdot \mathbf{v}^i. \quad (3.3)$$

With $\mathbf{f}^{ij} = -\mathbf{f}^{ji}$ and the identity of localization function $\psi(\mathbf{x})$,[24,28]

$$\psi(\mathbf{r}^k - \mathbf{x}) - \psi(\mathbf{r}^l - \mathbf{x}) = -\mathbf{r}^{kl} \cdot \nabla_{\mathbf{x}} \int_0^1 \psi(\mathbf{r}^k \lambda + \mathbf{r}^l (1-\lambda) - \mathbf{x}) \mathrm{d}\lambda, \quad (3.4)$$

$$\begin{aligned} &\sum_i \sum_{j\neq i} \mathbf{f}^{ij} \psi(\mathbf{r}^i - \mathbf{x}) \\ &= \frac{1}{2} \sum_i \sum_{j\neq i} \mathbf{f}^{ij} (\psi(\mathbf{r}^i - \mathbf{x}) - \psi(\mathbf{r}^j - \mathbf{x})) \\ &= -\mathrm{div} \left\{ \frac{1}{2} \sum_i \sum_{j\neq i} \mathbf{f}^{ij} \otimes \mathbf{r}^{ij} \int_0^1 \psi(\mathbf{r}^i \lambda + \mathbf{r}^j (1-\lambda) - \mathbf{x}) \mathrm{d}\lambda \right\}, \end{aligned} \quad (3.5)$$

where the symbol $\otimes$ represents tensor product. Using $\nabla_{\mathbf{r}^i} \psi(\mathbf{r}^i - \mathbf{x}) = -\nabla_{\mathbf{x}} \psi(\mathbf{r}^i - \mathbf{x})$ we have

$$m^i \mathbf{v}^i \frac{\partial \psi(\mathbf{r}^i - \mathbf{x})}{\partial \mathbf{r}^i} \cdot \mathbf{v}^i = -m^i \mathbf{v}^i \frac{\partial \psi(\mathbf{r}^i - \mathbf{x})}{\partial \mathbf{x}} \cdot \mathbf{v}^i = -\mathrm{div} \left\{ \sum_i m^i \mathbf{v}^i \otimes \mathbf{v}^i \psi(\mathbf{r}^i - \mathbf{x}) \right\}. \quad (3.6)$$

The relative velocity of a particle, $\tilde{\mathbf{v}}^i$, with respect to the continuum velocity is defined as

$$\tilde{\mathbf{v}}^i := \mathbf{v}^i - \mathbf{v}. \quad (3.7)$$

Therefore Eq. (3.6) can be rewritten as

$$m^i \mathbf{v}^i \frac{\partial \psi(\mathbf{r}^i - \mathbf{x})}{\partial \mathbf{r}^i} \cdot \mathbf{v}^i = -\mathrm{div} \left\{ \sum_i m^i \tilde{\mathbf{v}}^i \otimes \tilde{\mathbf{v}}^i \psi(\mathbf{r}^i - \mathbf{x}) \right\} - \mathrm{div} \{\rho \mathbf{v} \otimes \mathbf{v}\}, \quad (3.8)$$

where $\sum_i m^i \tilde{\mathbf{v}}^i \otimes \mathbf{v} \psi(\mathbf{r}^i - \mathbf{x}) = 0$ has been used. From Eqs. (3.2), (3.5), and (3.8), the equation of motion from the atomistic perspective is given by

$$\begin{aligned} &\frac{\partial(\rho \mathbf{v})}{\partial t} + \mathrm{div}(\rho \mathbf{v} \otimes \mathbf{v}) \\ &= \mathrm{div} \left\{ -\sum_i m^i \tilde{\mathbf{v}}^i \otimes \tilde{\mathbf{v}}^i \psi(\mathbf{r}^i - \mathbf{x}) \right. \\ &\quad \left. -\frac{1}{2} \sum_i \sum_{j\neq i} \mathbf{f}^{ij} \otimes \mathbf{r}^{ij} \int_0^1 \psi(\mathbf{r}^i \lambda + \mathbf{r}^j (1-\lambda) - \mathbf{x}) \mathrm{d}\lambda \right\}. \end{aligned} \quad (3.9)$$

On the other hand, equation of motion from continuum mechanics[37] is

$$\frac{\partial(\rho \mathbf{v})}{\partial t} + \mathrm{div}\{\rho \mathbf{v} \otimes \mathbf{v}\} = \mathrm{div}\boldsymbol{\sigma}. \quad (3.10)$$

Comparing Eq. (3.9) and (3.10), it is apparent that

$$\begin{aligned} \boldsymbol{\sigma}^h = &-\sum_i m^i \tilde{\mathbf{v}}^i \otimes \tilde{\mathbf{v}}^i \psi(\mathbf{r}^i - \mathbf{x}) \\ &-\frac{1}{2} \sum_i \sum_{j\neq i} \mathbf{f}^{ij} \otimes \mathbf{r}^{ij} \int_0^1 \psi(\mathbf{r}^i \lambda + \mathbf{r}^j (1-\lambda) - \mathbf{x}) \mathrm{d}\lambda. \end{aligned} \quad (3.11)$$

The superscript h indicates the pointwise stress tensor $\boldsymbol{\sigma}$ is obtained through Hardy's formulism. Because $\mathbf{f}^{ij} := -\frac{\partial E_V}{\partial \mathbf{r}^{ij}}$ is parallel to $\mathbf{r}^{ij}$, the potential component of $\boldsymbol{\sigma}_V^h$ is symmetric, as is the kinetic component of $\boldsymbol{\sigma}_K^h$.

Substituting the expression of $\mathbf{f}^{ij}$ (Eq. (2.7)) for the polymer system into $\boldsymbol{\sigma}_V^h$, we have

$$\boldsymbol{\sigma}_V^h = -\frac{1}{2} \sum_i \sum_{j\neq i} \left\{ \mathbf{f}_{stretch}^{ij} + \mathbf{f}_{LJ}^{ij} + \sum_k \mathbf{f}_{bend}^{ij} + \ldots + \frac{1}{2} \sum_k \sum_{l\neq k} \mathbf{f}_{torsion}^{ij} \right\} \otimes \mathbf{r}^{ij} B(\mathbf{x}; \mathbf{r}^i, \mathbf{r}^j), \quad (3.12)$$

where $B(\mathbf{x}; \mathbf{r}^i, \mathbf{r}^j) := \int_0^1 \psi(\mathbf{r}^i \lambda + \mathbf{r}^j (1-\lambda) - \mathbf{x}) \mathrm{d}\lambda$.

IV. STRESS CALCULATION FROM MOLECULAR DYNAMICS SIMULATION

Hardy stress is computed for a coarse-grained (CG) polyethylene (PE) model modeled by multi-body potentials. Though details of the CG model has been described in other studies,[33,34,38] here we will briefly review some main features for completeness. Each CH_2 is treated as a superatom, having a mass of 14 u. We use the same superatom to represent the CH_3 group at the end of the chain. The superatoms are interacting through the potentials described in Eq. (2.1), and the parameters for the force field of the CG PE can be found in previous work.[33,34,39] PE polymer systems consisting of a single chain having 1000 superatoms per chain (Fig. 1) and 100 chains each having 10 superatoms are generated at 500 K using the excluded volume method,[40] with an initial density of around 0.5 g cm^{-3}. The excluded volume method[40] ensures that the generated PE configuration is energetically

preferable. The PE polymer samples as prepared are relaxed under NPT condition for 500 ps at 500 K and with an applied isotropic zero pressure using MD simulation. A Nose/Hoover barostat and thermostat is applied to keep the pressure and temperature constant, respectively. Configurations at lower temperatures are generated by cooling the samples from 500 K to lower temperature in a stepwise manner with the effective cooling rate of 50 K ns^{-1}. A timestep size of 1 fs is employed throughout our MD simulation. All the MD simulations are performed using LAMMPS.[41] The snapshots for visualization are generated using VMD graphics package.[42]

Hardy stress expression (Eq. (3.12)) is employed to compute the stress distribution in PE polymers. Since we consider equilibrium conditions in this section, time averaging[25] is applied to investigate the convergence of the computed Hardy stress, which is calculated every 100 timesteps. Two types of the localization functions are considered:

$$\psi_1(r) = \begin{cases} \dfrac{15}{4\pi R_c^3}\left\{1 - 3\left(\dfrac{r}{R_c}\right)^2 + 2\left(\dfrac{r}{R_c}\right)^3\right\} & \text{if } r = |\mathbf{x}_\alpha - \mathbf{x}| < R_c \\ 0 & \text{otherwise} \end{cases}, \tag{4.1a}$$

$$\psi_2(r) = \begin{cases} c & \text{if } r \le R_c - \delta \\ \dfrac{1}{2}c\left(1 - \cos\left(\dfrac{R_c - r}{\delta}\pi\right)\right) & \text{if } R_c - \delta < r \le R_c \\ 0 & \text{otherwise} \end{cases}, \tag{4.1b}$$

where $c = 1/4\pi(\frac{1}{6}R_c^3 + \frac{1}{6}(R_c - \delta)^3 - \frac{\delta^2}{\pi^2}(2R_c - \delta))$ to keep $\psi_2(r)$ normalized. Both functions satisfy the desired characteristic set by Hardy:[15] (a) $\psi(\mathbf{x} - \mathbf{r}^i)$ has its maximum at $\mathbf{r}^i = \mathbf{x}$; (b) $\psi(\mathbf{x} - \mathbf{r}^i) \to 0$ as $|\mathbf{x} - \mathbf{r}^i| \to \infty$; (c) $\psi(\mathbf{x} - \mathbf{r}^i)$ is smooth and non-negative; (d) $\int_{R^3} \psi(\mathbf{x} - \mathbf{r}^i)\mathrm{d}^3\mathbf{x} = 1$. From Fig. 2, it can be observed that the shape of $\psi_2(r)$ can be adjusted by changing the value of δ; note that when $r = R_c$, $\psi_1(r)$ is almost identical with $\psi_2(r)$. In this study, various radii of the spatial averaging volume, R_c, are also considered to test its effect on the convergence of Hardy stress. Hardy stress expression has been demonstrated to obey the balance of momentum (Eq. (3.10)) in Sec. III. Here we also test the conservation of momentum numerically using the computed Hardy's density (Eq. (3.1a)), velocity (Eq. (3.1c)), and stress (Eq. (3.12)) for the polymer system.[26,27] Using the finite difference method, the discretized version of (3.10) without considering body force is given by

$$\begin{aligned} &\rho\frac{v_\alpha^{(j+1)} - v_\alpha^{(j)}}{\delta t} + \rho\left\{\frac{v_\alpha^{(i+1)} - v_\alpha^{(i)}}{\delta x}v_x\right. \\ &\left. + \frac{v_\alpha^{(k+1)} - v_\alpha^{(k)}}{\delta y}v_y + \frac{v_\alpha^{(m+1)} - v_\alpha^{(m)}}{\delta z}v_z\right\} \\ &= \frac{\sigma_{\alpha x}^{(i+1)} - \sigma_{\alpha x}^{(i)}}{\delta x} + \frac{\sigma_{\alpha y}^{(k+1)} - \sigma_{\alpha y}^{(k)}}{\delta y} + \frac{\sigma_{\alpha z}^{(m+1)} - \sigma_{\alpha z}^{(m)}}{\delta z} \\ &(\alpha = x, y, z) \end{aligned} \tag{4.2}$$

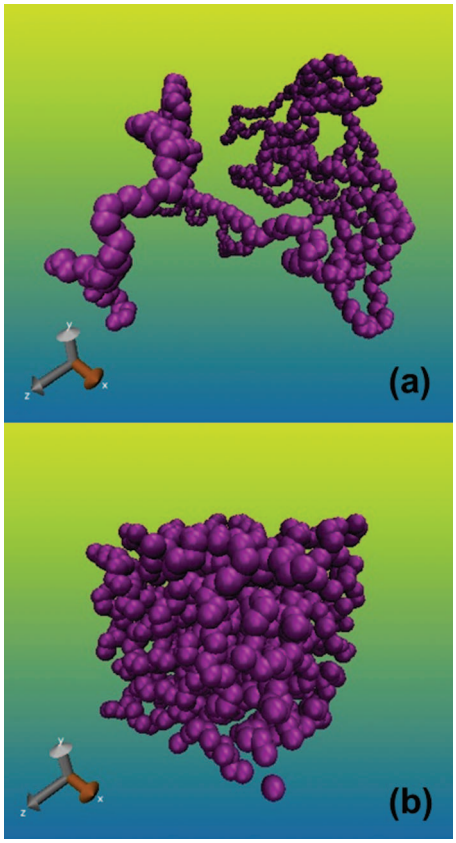

FIG. 1. Snapshots of single PE polymer chain equilibrated at 300 K at (a) unfolded state and (b) folded state with the constraint of periodic boundary condition.

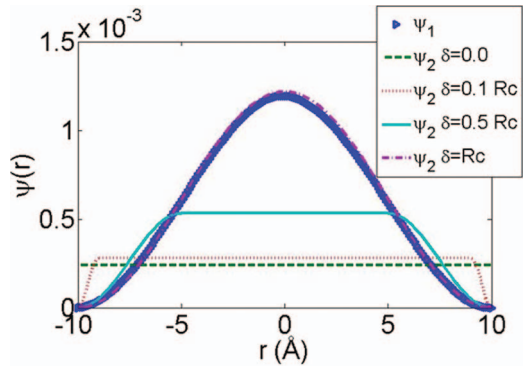

FIG. 2. Localization function $\psi_1(r)$ and $\psi_2(r)$ with varying δ at $R_c = 10$ Å (Eq. (4.1)).

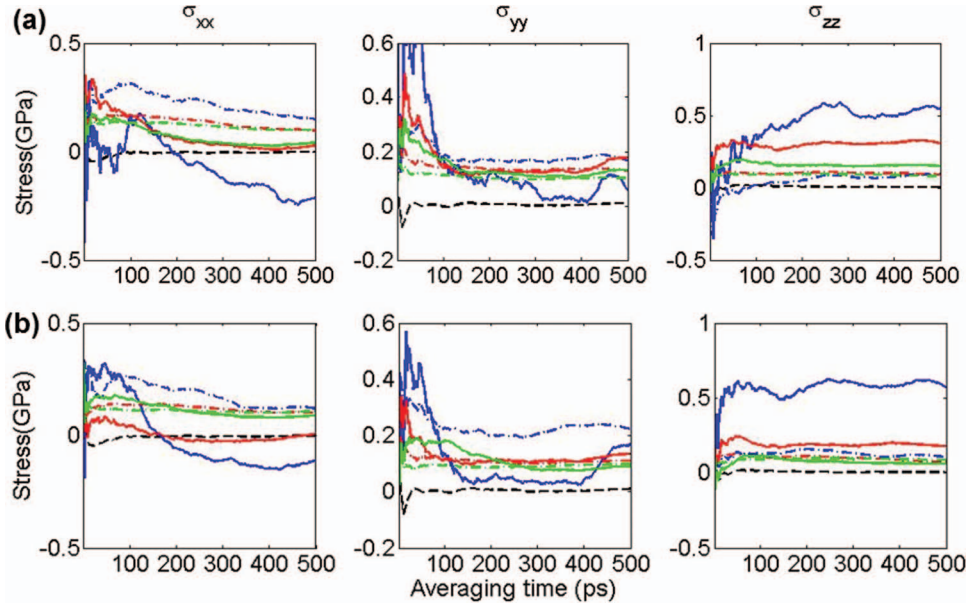

FIG. 3. Variation of stress components with averaging time window size for the polymer system at 300 K and zero pressure computed using (a) $\psi_1(r)$ and (b) $\psi_2(r)$ with $\delta = 0.1\ R_c$ at $R_c = 3$ Å (blue), $R_c = 6$ Å (red), and $R_c = 6$ Å (green). The Stress computed from a random point is in solid line; the averaged stress is in dashed line.

Here, $\sigma_{xx}^{(ikmj)}$ represents $\sigma_{xx}(x_i, y_k, z_m, t_j)$ and similarly for $\rho^{(ikmj)}$ and $\mathbf{v}^{(ikmj)}(v_\alpha^{(ikmj)})$. For simplicity, superscript is not explicitly written at (x_i, y_k, z_m, t_j) if not necessary. For example, $\sigma_{xx}^{((i+1)kmj)}$ is written as $\sigma_{xx}^{(i+1)}$. $\delta x = x_{i+1} - x_i$, $\delta y = y_{k+1} - y_k$, $\delta z = z_{m+1} - z_m$, and $\delta t = t_{j+1} - t_j$. δt is chosen to be 0.1 fs and $\delta x = \delta y = \delta z = 0.05$ Å. Hardy's density, velocity, and stress are computed in terms of atomic variables at chosen spatial points (x_i, y_k, z_m) and time instants, t_j, using Hardy's formulas. The agreement between the two sides of the balance laws are tested by plotting the left hand side (LHS) and right hand side (RHS) of the equations. Throughout this paper, only the momentum conservation in x direction is considered; LHS of the balance of momentum is presented in solid line while RHS in dashed line.

Figure 1 shows the PE system with periodic boundary conditions applied to all directions. The size of the system is around 31.15 Å × 31.15 Å × 31.15 Å. The system has been well equilibrated at 300 K and zero stress. The polymer is in melt state at 300 K. The computed stress at a random chosen time instant fluctuates as the continuum spatial point moving in the x direction along the centerline of the PE polymer system, and the fluctuation amplitude becomes lower as the spatial averaging volume gets larger. Comparison between Hardy stress with different averaging volumes and virial stress is plotted in Fig. 3. Virial stress of the PE system is computed using the definition of $\mathbf{f}^{ij}$ in Eq. (2.7),

$$\sigma^V = -\frac{1}{V}\left\{\sum_i m^i \mathbf{v}^i \otimes \mathbf{v}^i + \frac{1}{2}\sum_i \sum_{j\neq i} \mathbf{f}^{ij} \otimes \mathbf{r}^{ij}\right\}, \quad (4.3)$$

where V is the system volume. Hardy stress is computed at up to 8 randomly chosen spatial points in the PE system using both types of localization function in Eq. (4.1). $\delta = 0.1R_c$ is chosen for $\psi_2(r)$ so that $\psi_1(r)$ and $\psi_2(r)$ have distinctive shapes and the influence of the localization function can be further studied. It can be seen that the radius of spatial averaging volume R_c can influence the convergence of Hardy stress significantly. While stress mostly converges after averaging over 500 ps at $R_c = 6$ Å and 9 Å, the stress computed

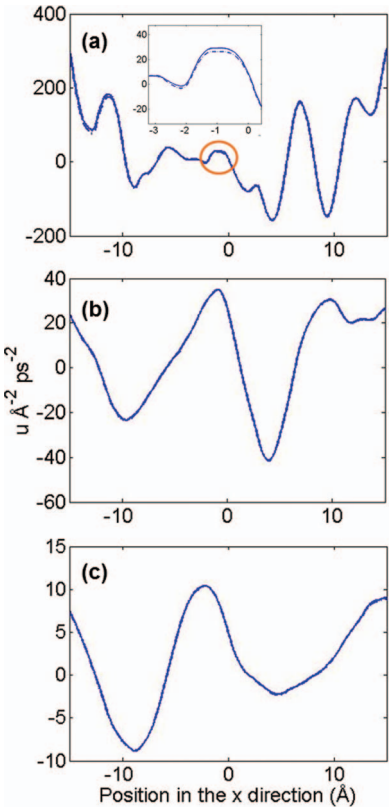

FIG. 4. Balance of momentum for the polymer system at 300 K and zero pressure computed using $\psi_1(r)$ with R_c equals to (a) 3 Å, (b) 6 Å, and (c) 9 Å (Solid curves are computed from the LHS of Eq. (4.2) and dotted curves are from the RHS).

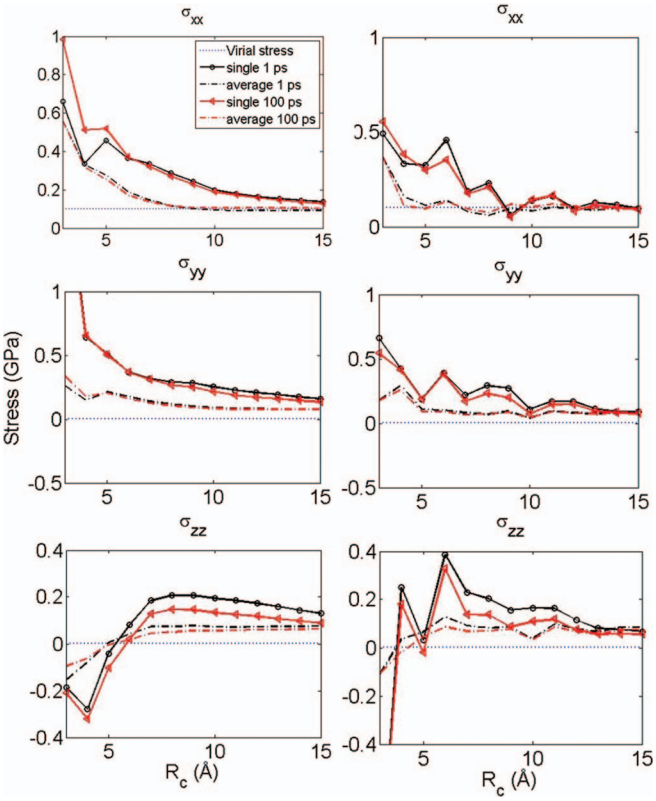

FIG. 5. Variation of stress components computed using $\psi_1(r)$ (left column) and $\psi_2(r)$ (right column) with $\delta = 0.1\ R_c$ averaged over different time window size with increasing R_c for the polymer system of chain length 1000 tensile strained to 8% at 25 K.

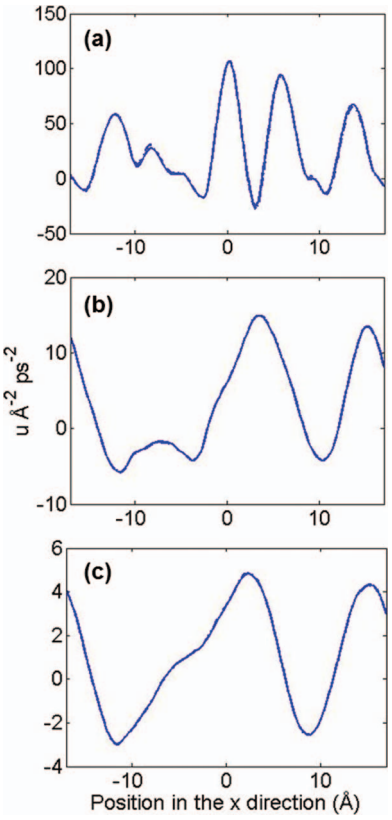

FIG. 6. Balance of momentum for the polymer system of chain length 10 tensile strained to 8% at 25 K computed with R_c equals to (a) 3 Å, (b) 6 Å, and (c) 9 Å.

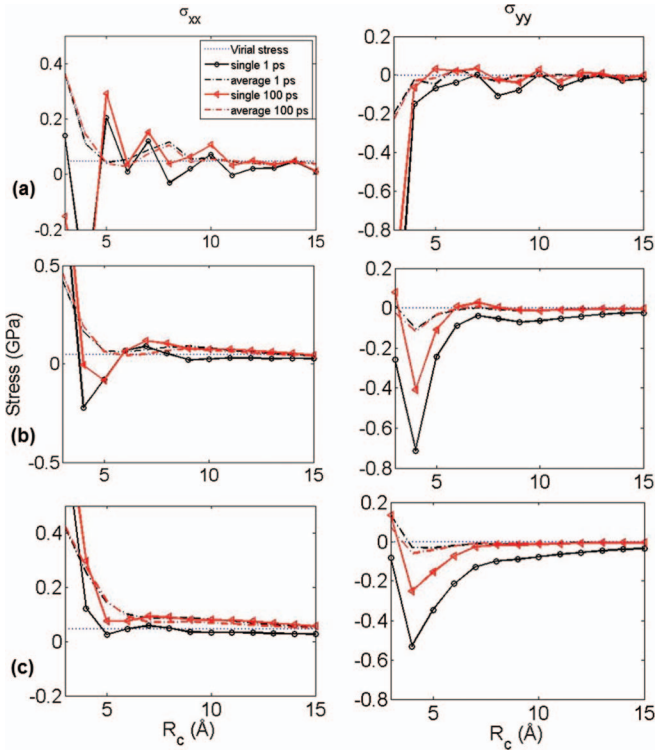

FIG. 7. Variation of stress components computed using $\psi_2(r)$ with (a) $\delta = 0.1\ R_c$, (b) $\delta = 0.5\ R_c$, and (c) $\delta = R_c$ averaged over various time steps with increasing R_c for the polymer system of chain length 10 tensile strained to 8% at 25 K.

with $R_c = 3$ Å still shows large fluctuations for a randomly chosen single point. Averaged stress over 8 points (dashed lines) demonstrates improved convergence as revealed by the smoother and more flat curves. It can also been observed that stress computed with different R_c converge to different values instead of the system averaged virial stress, even after averaging over multiple spatial points. This is mainly because Hardy's expression provides an estimate of local stress at the chosen spatial point, and the averaging time window is not large enough for the polymer chain to move through all configurations. Thus the local stress at the spatial points can diverge from the system average and larger spatial averaging volume as well as averaging over more spatial points are necessary because of the inhomogeneous nature of polymer system. Stress computed with different forms of the localization function have certain differences, but little effect of the localization function has been observed for the averaged stress over multiple points computed at large R_c. The balance of momentum is obeyed by the computed Hardy's density, velocity, and stress, as demonstrated by the good agreement between LHS and RHS of Eq. (4.2) using $\psi_1(r)$ (Fig. 4). The momentum conservation holds for different spatial averaging volume, irrespective of the specific form of the localization function. Results from $\psi_2(r)$ with $\delta = 0.1R_c$ are not shown here mainly due to the noise in the balance of momentum plot resulted from reduced smoothness of $\psi_2(r)$ compared with $\psi_1(r)$ (Fig. 2). Since Hardy's definition of density and velocity is not as controversial as stress, the validity of balance of momentum justifies the application of the Hardy stress expression to multi-body potential systems.The PE system is

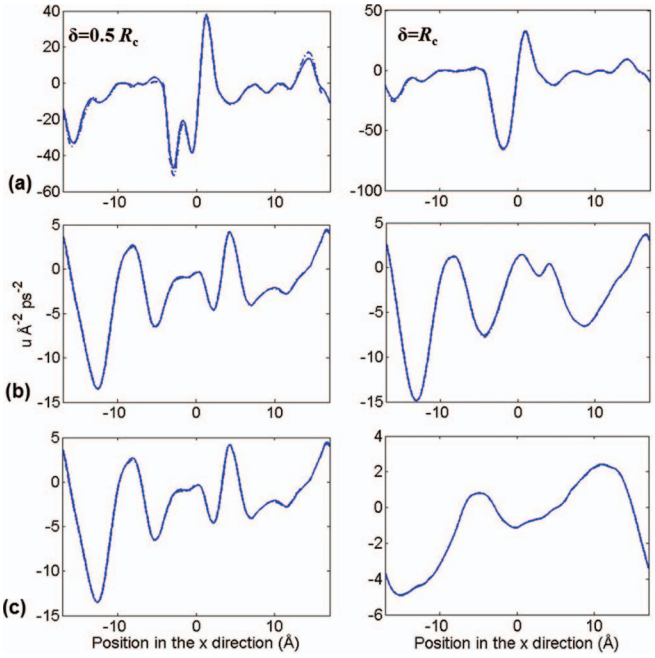

FIG. 8. Balance of momentum for the polymer system of chain length 10 tensile strained to 8% at 25 K computed using $\psi_2(r)$ at $\delta = 0.5\ R_c$ (left column) and $\delta = R_c$ (right column) with R_c equals to (a) 3 Å, (b) 6 Å, and (c) 9 Å.

then deformed in the x direction by applying 8% uniaxial tensile strain at 25 K, while the lateral dimensions (in y and z directions) are controlled by the barostat to keep constant zero stress. The polymer is in glassy state at 25 K. PE systems with different chain length 1000 and 10 are considered in the tensile test, both having a total of 1000 superatoms. Similarly, stress varies as the spatial point moves from one periodic boundary of the PE system to the other boundary along the x direction at a random chosen time instant. The fluctuation diminishes with increasing spatial averaging volume. The stress computed with $R_c = 9$ Å approaches the system average computed by virial stress ($\sigma_{xx} = 101.4$ MPa) for the polymer system of chain length 1000. The influence of R_c and averaging time window size for the polymer chain of length 1000 is shown in Fig. 5. Since the system is equilibrated at comparably low temperature (25 K), the effect of averaging time window size is not significant, as demonstrated by little difference between averaging over 1 ps and 100 ps. Computed σ_{xx} gradually converges to the system average with increasing R_c, while σ_{yy} and σ_{zz} diverge a little from the virial stress (Fig. 5). Averaging over multiple spatial points (dashed lines) can lead to better convergence. Computed stress with $\psi_1(r)$ varies smoothly with increasing R_c, in contrast to that computed with $\psi_2(r)$, which should be ascribed to the relatively sharpness of $\psi_2(r)$. Note that the difference between the stress computed with different localization functions reduce at large spatial averaging volume. The balance of momentum is also validated by comparing two sides of Eq. (4.2) numerically, and the good agreement again justifies the validity of Hardy stress expression for multi-body potential system (Fig. 6). The convergence of stress with R_c computed using $\psi_2(r)$ with different δ for the polymer chain of length 10 is shown in Fig. 7. The convergence curves apparently become smoother

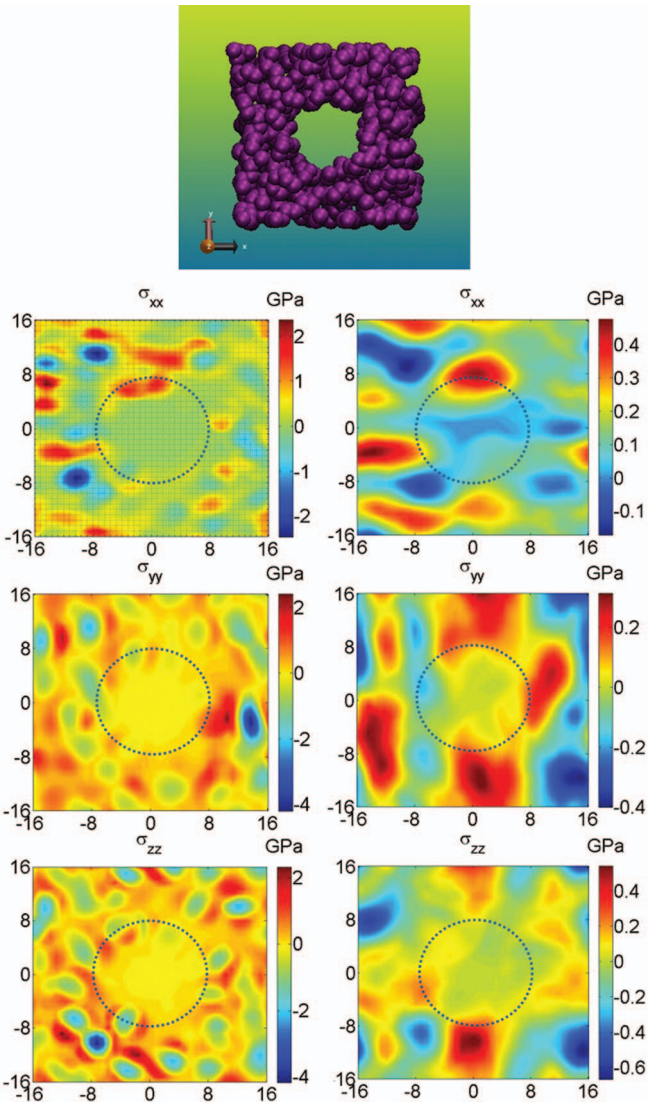

FIG. 9. Stress distribution of the polymer system (purple spheres represent superatoms) with a center hole tensile strained to 8% at 25 K computed with R_c equals to 3 Å (left column) and (b) 6 Å (right column).

with increasing δ as $\psi_2(r)$ become less sharp. All of the averaged stress over multiple points with different localization functions are converged to the system averaged values as R_c increases. A spatial averaging volume of $R_c = 10$ Å can lead to relatively good approximation. Again, note that the balance of momentum can be established with different values of δ and various R_c (Fig. 8).

A center hole is created in the PE system and applied with the same deformation protocol to 8% strain in the x direction at 25 K. Hardy stress at the x-y coordinate plane is computed using $\psi_1(r)$ at the grid points shown in Fig. 8(a), and the dashed circle represents the center hole estimated by the position of polymer superatoms at inner surface. The stress is averaged over 1 ps because thermal fluctuation is relatively small at 25 K (Figs. 5 and 7). Stress can be non-zero even in the hole, because the atoms outside the spatial averaging volume could also contribute to the potential part of Hardy stress at the chosen spatial point (Eq. (3.12)). One can easily observe the non-uniform stress distribution on the center plane while the PE system is stretched along the x direction. The

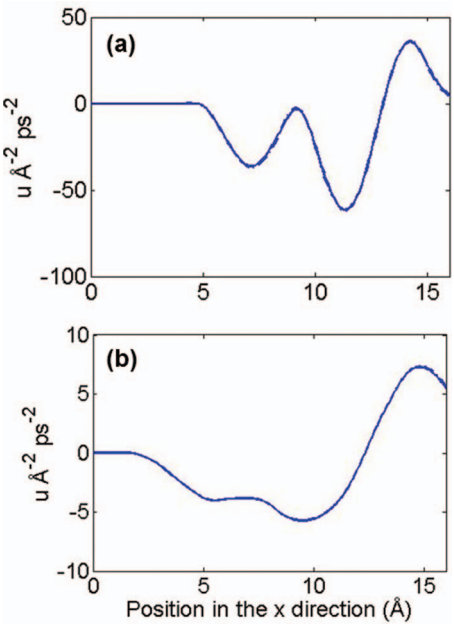

FIG. 10. Balance of momentum for the polymer system with a center hole tensile strained to 8% at 25 K computed with R_c equals to (a) 3 Å and (b) 6 Å.

stress fluctuations smear out if spatial averaging volume is increased, but the non-uniform stress distribution is still pronounced (Fig. 9). Balance of momentum is tested along centerline in the x direction, and can be still established in this case, as shown in Fig. 10 where the two sides of Eq. (4.2) are identical.

V. CONCLUSION

Stress definition for multi-body potential systems has been a controversial topic for decades. Among the limited attempts to address this problem, Admal *et al.*[31,32] demonstrated that the force on a particle can always be decomposed as a sum of central forces between particles for most practical interatomic potentials, and thus symmetric microscopic stress tensors can be derived. Chen[28] also demonstrated the invariance of Hardy stress formula for three-body systems with $\mathbf{f}^{ij} := -\partial E_V/\partial \mathbf{r}^{ij}$, consistent with the force decomposition formula proposed by Admal *et al.* In this work, we investigated the extension of Hardy stress expression to a polymer system described by multi-body potentials including bending angle and torsional angle, with central force decomposition $\mathbf{f}^i = -\frac{\partial E_V}{\partial \mathbf{r}^i} = -\sum_j \frac{\partial E_V}{\partial r^{ij}} \frac{\mathbf{r}^{ij}}{r^{ij}} = \sum_j \mathbf{f}^{ij}$. Through simple PE polymer systems equilibrated at finite temperature, we found that Hardy's density, velocity, and stress obey balance of momentum both theoretically and numerically. Since Hardy's density and velocity are not directly related to the specific form of interatomic potentials of the system, the validity of momentum conservation provides justification to the extension of Hardy stress expression to the multi-body potential system. Balance of momentum has been demonstrated to hold for the PE system of different chain length, at zero pressure and under deformation, with and without a center hole. Stress distribution has been found to be highly non-uniform within the PE system even at equilibrium state, and only converge to the system average computed by virial stress at large spatial averaging volume. Averaging over multiple spatial points can significantly improve the convergence. Specific choice of the localization function affects the computed stress only at relatively small spatial volume and before averaging over different spatial points. Even though we demonstrate the validity of Hardy stress expression for simple polymer systems, the conclusion should also be applied to general multi-body potential systems. The non-uniqueness of stress tensor caused by multiple possible force decomposition is not included in the present study and will be addressed by the authors in future.

ACKNOWLEDGMENTS

The authors gratefully acknowledge the support of the Office of Naval Research under Grant No. N00014-13-1-0386.

APPENDIX: CENTRAL FORCE EXPRESSIONS FOR THE BENDING AND TORSIONAL POTENTIALS

In this section, we present central force expressions for the commonly used interatomic potential energy for polymers including bond stretching, bending, torsional, and non-bonded terms (Eq. (2.1)). Since the potentials that describe bond stretching and non-bonded terms are pairwise, we only present the derivations for bending and torsional terms in the interatomic potentials.

1. Central force expression due to bending deformation

Consider sequent three atoms (atoms i, j, k) in a polymer chain with bond angle equals θ_{ijk}, where pairs (i, j) and (j, k) are covalently bonded. The interatomic potential from bending deformation is

$$V_\theta(r^{ij}, r^{ik}, r^{jk}) = k_\theta(\cos\theta^{ijk} - \cos\theta_0)^2 = k_\theta\left(\frac{(r^{ij})^2 + (r^{kj})^2 - (r^{ik})^2}{2r^{ij}r^{kj}} - \cos\theta_0\right)^2, \tag{A1}$$

where $\cos\theta^{ijk} = \frac{\mathbf{r}^{ij}\cdot\mathbf{r}^{kj}}{r^{ij}r^{kj}}$, k_θ is the constant for bond bending potential, θ_0 is the equilibrium bond angle, $\mathbf{r}^{ij} = \mathbf{r}^i - \mathbf{r}^j$, $r^{ij} = |\mathbf{r}^{ij}|$.

The interatomic force between atoms i and j is defined as $\mathbf{f}^{ij} := -\frac{\partial E_V}{\partial r^{ij}}\hat{\mathbf{r}}^{ij}$, $\hat{\mathbf{r}}^{ij}$ is the unit vector along $\mathbf{r}^{ij}$. Thus the pair force between atoms i and j from bending potential is given by

$$\mathbf{f}^{ij}_{bend} = -\frac{\partial V_\theta}{\partial r^{ij}}\hat{\mathbf{r}}^{ij} = -2k_\theta\left(\cos\theta^{ijk} - \cos\theta_0\right)\left(\frac{1}{r^{jk}} - \frac{\cos\theta^{ijk}}{r^{ij}}\right)\hat{\mathbf{r}}^{ij}. \tag{A2}$$

Similarly, the central force between atom pairs (i, k) and (j, k) are, respectively,

$$\mathbf{f}_{bend}^{ik} = -\frac{\partial V_\theta}{\partial r^{ik}}\hat{\mathbf{r}}^{ik} = 2k_\theta(\cos\theta^{ijk} - \cos\theta_0)\frac{r^{ik}}{r^{ij}r^{kj}}\hat{\mathbf{r}}^{ik}, \quad \text{(A3)}$$

$$\mathbf{f}_{bend}^{jk} = -2k_\theta(\cos\theta^{ijk} - \cos\theta_0)\left(\frac{1}{r^{ij}} - \frac{\cos\theta^{ijk}}{r^{kj}}\right)\hat{\mathbf{r}}^{jk}. \quad \text{(A4)}$$

2. Central force expression due to torsional deformation

Consider sequent four atoms (atoms i, j, k, l) in a polymer chain with dihedral angle equals ϕ^{ijkl}, where pairs (i, j), (j, k), (k, l) are covalently bonded. The interatomic potential from torsional deformation is

$$V_\phi(r^{ij}, r^{ik}, \ldots r^{kl}) = c_0 + c_1\cos\phi^{ijkl} + c_2\cos^2\phi^{ijkl} + c_3\cos^3\phi^{ijkl} + c_4\cos^4\phi^{ijkl},$$

$$\cos\phi^{ijkl} = \frac{(\mathbf{r}^{kj}\times\mathbf{r}^{ik})\cdot(\mathbf{r}^{kj}\times\mathbf{r}^{lk})}{\|\mathbf{r}^{kj}\times\mathbf{r}^{ik}\|\|\mathbf{r}^{kj}\times\mathbf{r}^{lk}\|} = \frac{(\mathbf{r}^{ik}\cdot\mathbf{r}^{lk})(\mathbf{r}^{kj})^2 - (\mathbf{r}^{ik}\cdot\mathbf{r}^{kj})(\mathbf{r}^{kj}\cdot\mathbf{r}^{lk})}{\|\mathbf{r}^{kj}\times\mathbf{r}^{ik}\|\|\mathbf{r}^{kj}\times\mathbf{r}^{lk}\|}$$

$$= \frac{\cos\theta^{ikl} - \cos\theta^{ikj}\cos\theta^{jkl}}{(1-\cos\theta^{ikj})^{1/2}(1-\cos\theta^{jkl})^{1/2}}, \quad \text{(A5)}$$

where c_n ($n = 0, 1, 2, 3, 4$) are the constants of torsional potential:

$$\mathbf{f}_{torsion}^{ij} = -\frac{\partial V_\phi}{\partial r^{ij}}\hat{\mathbf{r}}^{ij} = -\frac{\mathrm{d}V_\phi}{\mathrm{d}\cos\phi^{ijkl}}\frac{\partial\cos\phi^{ijkl}}{\partial r^{ij}}\hat{\mathbf{r}}^{ij}. \quad \text{(A6)}$$

The derivative of V_ϕ with respect to $\cos\phi^{ijkl}$ is given by

$$f_\phi^{ijkl} = \frac{\mathrm{d}V_\phi}{d\cos\phi^{ijkl}} = c_1 + 2c_2\cos\phi^{ijkl} + 3c_3\cos^2\phi^{ijkl} + 4c_4\cos^3\phi^{ijkl}. \quad \text{(A7)}$$

And the partial derivative of $\cos\phi^{ijkl}$ with respect to r^{ij} is given by

$$\frac{\partial\cos\phi^{ijkl}}{\partial r^{ij}} = \frac{\partial\cos\phi^{ijkl}}{\partial\cos\theta^{ikj}}\frac{\partial\cos\theta^{ikj}}{\partial r^{ij}} = \left(\frac{\cos\theta^{jkl}}{\sin\theta^{ikj}\sin\theta^{jkl}} - \cos\phi^{ijkl}\frac{\cos\theta^{ikj}}{\sin^2\theta^{ikj}}\right)\frac{r^{ij}}{r^{ik}r^{jk}} \quad \text{(A8)}$$

Substituting Eqs. (A7) and (A8) into Eq. (A6), we obtain

$$\mathbf{f}_{torsion}^{ij} = -f_\phi^{ijkl}\left(\frac{\cos\theta^{jkl}}{\sin\theta^{ikj}\sin\theta^{jkl}} - \cos\phi^{ijkl}\frac{\cos\theta^{ikj}}{\sin^2\theta^{ikj}}\right)\frac{r^{ij}}{r^{ik}r^{jk}}\hat{\mathbf{r}}^{ij} \quad \text{(A9)}$$

Similarly, the central force between atom pairs (i, k), (i, l), (j, k), (j, l), and (k, l) are, respectively,

$$\mathbf{f}_{torsion}^{ik} = -f_\phi^{ijkl}\left(\frac{1}{\sin\theta^{ikj}\sin\theta^{jkl}}\left(\frac{1}{r^{kl}} - \frac{\cos\theta^{jkl}}{r^{jk}}\right) + \frac{\cos\phi^{ijkl}}{\sin^2\theta^{ikj}}\left(\frac{\cos\theta^{ikj}}{r^{jk}} - \frac{1}{r^{ik}}\right)\right)\hat{\mathbf{r}}^{ik}, \quad \text{(A10)}$$

$$\mathbf{f}_{torsion}^{il} = f_\phi^{ijkl}\frac{1}{\sin\theta^{ikj}\sin\theta^{jkl}}\frac{r^{il}}{r^{ik}r^{kl}}\hat{\mathbf{r}}^{il}, \quad \text{(A11)}$$

$$\mathbf{f}_{torsion}^{jk} = -f_\phi^{ijkl}\left(\begin{array}{l}\dfrac{1}{\sin\theta^{ikj}\sin\theta^{jkl}}\left(-\dfrac{\cos\theta^{jkl}}{r^{ik}} - \dfrac{\cos\theta^{ikj}}{r^{kl}} + \dfrac{2\cos\theta^{ikj}\cos\theta^{jkl}}{r^{jk}}\right)\\ +\cos\phi^{ijkl}\left(\dfrac{\cos\theta^{ikj}}{\sin^2\theta^{ikj}}\left(\dfrac{1}{r^{ik}} - \dfrac{\cos\theta^{ikj}}{r^{jk}}\right) + \dfrac{\cos\theta^{jkl}}{\sin^2\theta^{jkl}}\left(\dfrac{1}{r^{kl}} - \dfrac{\cos\theta^{jkl}}{r^{jk}}\right)\right)\end{array}\right)\hat{\mathbf{r}}^{jk}, \quad \text{(A12)}$$

$$\mathbf{f}_{torsion}^{jl} = -f_\phi^{ijkl}\left(\frac{\cos\theta^{ikj}}{\sin\theta^{ikj}\sin\theta^{jkl}} - \cos\phi^{ijkl}\frac{\cos\theta^{jkl}}{\sin^2\theta^{jkl}}\right)\frac{r^{jl}}{r^{jk}r^{kl}}\hat{\mathbf{r}}^{jl}, \quad \text{(A13)}$$

$$\mathbf{f}_{torsion}^{kl} = -f_\phi^{ijkl}\left(\frac{1}{\sin\theta^{ikj}\sin\theta^{jkl}}\left(\frac{1}{r^{ik}} - \frac{\cos\theta^{ikj}}{r^{jk}}\right) + \frac{\cos\phi^{ijkl}}{\sin^2\theta^{jkl}}\left(\frac{\cos\theta^{jkl}}{r^{jk}} - \frac{1}{r^{kl}}\right)\right)\hat{\mathbf{r}}^{kl}. \quad \text{(A14)}$$

[1]C. J. Kimmer and R. E. Jones, J. Phys.: Condens. Mater. **19**, 326207 (2007).
[2]P. A. Klein and J. A. Zimmerman, J. Comput. Phys. **213**, 86–116 (2006).
[3]V. B. Shenoy, R. Miller, E. b. Tadmor, D. Rodney, R. Phillips, and M. Ortiz, J. Mech. Phys. Solids **47**, 611–642 (1999).
[4]E. B. Tadmor, M. Ortiz, and R. Phillips, Philos. Mag. A **73**, 1529–1563 (1996).
[5]R. E. Rudd and J. Q. Broughton, Phys. Status Solidi B **217**, 251–291 (2000).
[6]L. E. Shilkrot, R. E. Miller, and W. A. Curtin, J. Mech. Phys. Solids **52**, 755–787 (2004).
[7]S. P. Xiao and T. Belytschko, Comput. Methods Appl. Mech. Eng. **193**, 1645–1669 (2004).
[8]J. Knap and M. Ortiz, J. Mech. Phys. Solids **49**, 1899–1923 (2001).
[9]W. E. B. Engquist, X. Li, W. Ren, and E. Vanden-Eijnden, Commun. Comput. Phys. **2**, 367–450 (2007).
[10]R. Clausius, Philos. Mag. 4 **40**, 122–127 (1870).
[11]J. C. Maxwell, Trans. R. Soc. Edinburgh **XXVI**, 1–43 (1870).
[12]J. C. Maxwell, Nature (London) **10**, 477–480 (1874).
[13]J. H. Irving and J. G. Kirkwood, J. Chem. Phys. **18**, 817–829 (1950).
[14]R. J. Hardy, J. Chem. Phys. **76**, 622–628 (1982).
[15]S. Root, R. J. Hardy, and D. R. Swanson, J. Chem. Phys. **118**, 3161–3165 (2003).
[16]A. I. Murdoch, Q. J. Mech. Appl. Math. **36**, 163–187 (1983).
[17]A. I. Murdoch and D. Bedeaux, Int. J. Eng. Sci. **31**, 1345–1373 (1993).
[18]A. I. Murdoch and D. Bedeaux, Proc. Royal Soc. London, Ser. A: Math. Phys. Engin. Sci. **445**, 157–179 (1994).
[19]A. I. Murdoch, "On the microscopic interpretation of stress and couple stress," in *The Rational Spirit in Modern Continuum Mechanics*, edited by C.-S. Man and R. Fosdick (Springer, Netherlands, 2004), pp. 599–625.
[20]A. I. Murdoch, J. Elasticity **88**, 113–140 (2007).
[21]R. E. Jones, J. A. Zimmerman, J. Oswald, and T. Belytschko, J. Phys.: Condens. Mater. **23**, 015002 (2011).
[22]H. U. Manfred, K. M. Kranthi, and P. Panayiotis, Modell. Simul. Mater. Sci. Eng. **21**, 015010 (2013).
[23]J. A. Zimmerman, R. E. Jones, and J. A. Templeton, J. Comput. Phys. **229**, 2364–2389 (2010).
[24]J. A. Zimmerman, E. B. WebbIII, J. J. Hoyt, R. E. Jones, P. A. Klein, and D. J. Bammann, Modell. Simul. Mater. Sci. Eng. **12**, S319 (2004).
[25]Y. Fu and A. C. To, Modell. Simul. Mater. Sci. Eng. **21**, 055015 (2013).
[26]Y. Fu and A. C. To, J. Appl. Phys. **113**, 233505 (2013).
[27]Y. Fu and A. C. To, Modell. Simul. Mater. Sci. Eng. **22**, 015010 (2014).
[28]Y. Chen, J. Chem. Phys. **124**, 054113 (2006).
[29]J. Tersoff, Phys. Rev. B **37**, 6991 (1988).
[30]F. H. Stillinger and T. A. Weber, Phys. Rev. B **31**, 5262–5271 (1985).
[31]N. Admal and E. B. Tadmor, J. Elasticity **100**, 63–143 (2010).
[32]N. C. Admal and E. B. Tadmor, J. Chem. Phys. **134**, 184106 (2011).
[33]D. Brown and J. H. R. Clarke, Macromolecules **24**, 2075–2082 (1991).
[34]F. M. Capaldi, M. C. Boyce, and G. C. Rutledge, Polymer **45**, 1391–1399 (2004).
[35]T. J. Delph, Modell. Simul. Mater. Sci. Eng. **13**, 585 (2005).
[36]J. W. Martin, J. Phys. C: Solid State Phys. **8**, 2837 (1975).
[37]L. E. Malvern, *Introduction to the Mechanis of a Continuous Medium* (Prentice-Hall, Upper Saddle River, 1969).
[38]Y. Li, M. Kröger, W. K. Liu, Macromolecules **45**, 2099–2112 (2012).
[39]Y. Fu and J.-H. Song, "Large deformation mechanism of glassy polyethylene polymer nanocomposites: Coarse grain molecular dynamics study," Comput. Mater. Sci. (in press).
[40]J. I. McKechnie, D. Brown, and J. H. R. Clarke, Macromolecules **25**, 1562–1567 (1992).
[41]See http://lammps.sandia.gov/ for LAMMPS Molecular Dynamics Simulator.
[42]See http://www.ks.uiuc.edu/Research/vmd/ for Visual Molecular Dynamics (VMD).